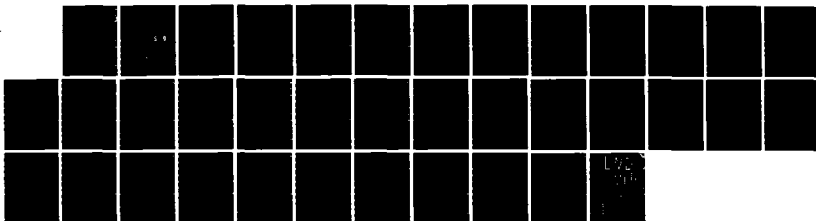


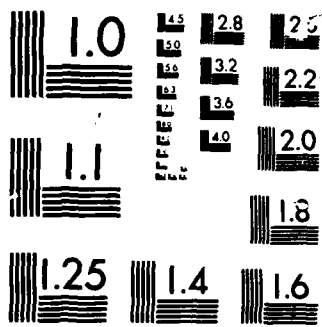
ND-A166 886 THE EFFECT OF FINITE 'BLOB' SIZE ON THE CURRENT
CONVECTIVE INSTABILITY IN THE AURORAL IONOSPHERE(U)
NAVAL RESEARCH LAB WASHINGTON DC J D HUBA ET AL.
UNCLASSIFIED 11 APR 86 NRL-MR-5739

1/1

F/G 4/1

NL





MICROCOPI

CHART

AD-A166 806

(2)

NRL Memorandum Report 5730

The Effect of Finite "Blob" Size on the Current Convective Instability in the Auroral Ionosphere

J. D. HUBA AND P. K. CHATURVEDI

*Geophysical and Plasma Dynamics Branch
Plasma Physics Division*

April 11, 1986

DTIC
ELECTED
MAY 06 1986
S D

This research was partially sponsored by the Defense Nuclear Agency under Subtask W99QMXWA, work unit 00010 and work unit title "Plasma Structure Evolution," and by the Office of Naval Research.



NAVAL RESEARCH LABORATORY
Washington, D.C.

Approved for public release; distribution unlimited.

86 5 5 082

DTIC FILE COPY

DISCLAIMER NOTICE

**THIS DOCUMENT IS BEST QUALITY
PRACTICABLE. THE COPY FURNISHED
TO DTIC CONTAINED A SIGNIFICANT
NUMBER OF PAGES WHICH DO NOT
REPRODUCE LEGIBLY.**

AD-A166806

SECURITY CLASSIFICATION OF THIS PAGE

REPORT DOCUMENTATION PAGE

1a. REPORT SECURITY CLASSIFICATION UNCLASSIFIED		1b. RESTRICTIVE MARKINGS																
2a. SECURITY CLASSIFICATION AUTHORITY		3. DISTRIBUTION/AVAILABILITY OF REPORT Approved for public release; distribution unlimited.																
2b. DECLASSIFICATION/DOWNGRADING SCHEDULE																		
4. PERFORMING ORGANIZATION REPORT NUMBER(S) NRL Memorandum Report 5730		5. MONITORING ORGANIZATION REPORT NUMBER(S)																
6a. NAME OF PERFORMING ORGANIZATION Naval Research Laboratory	6b. OFFICE SYMBOL (If applicable) Code 4780	7a. NAME OF MONITORING ORGANIZATION																
6c. ADDRESS (City, State, and ZIP Code) Washington, DC 20375-5000		7b. ADDRESS (City, State, and ZIP Code)																
8a. NAME OF FUNDING/SPONSORING ORGANIZATION DNA and ONR	8b. OFFICE SYMBOL (If applicable) RAAE	9. PROCUREMENT INSTRUMENT IDENTIFICATION NUMBER																
8c. ADDRESS (City, State, and ZIP Code) Washington, DC 20305 Arlington, VA 22217		10. SOURCE OF FUNDING NUMBERS <table border="1"><tr><td>PROGRAM ELEMENT NO. 63223C</td><td>PROJECT NO. RR033-02-44</td><td>TASK NO.</td><td>WORK UNIT ACCESSION NO. BR01043-000</td></tr></table>		PROGRAM ELEMENT NO. 63223C	PROJECT NO. RR033-02-44	TASK NO.	WORK UNIT ACCESSION NO. BR01043-000											
PROGRAM ELEMENT NO. 63223C	PROJECT NO. RR033-02-44	TASK NO.	WORK UNIT ACCESSION NO. BR01043-000															
11. TITLE (Include Security Classification) The Effect of Finite "Blob" Size on the Current Convective Instability in the Auroral Ionosphere																		
12. PERSONAL AUTHOR(S) Huba, J.D. and Chaturvedi, P.K.																		
13a. TYPE OF REPORT Interim	13b. TIME COVERED FROM _____ TO _____	14. DATE OF REPORT (Year, Month, Day) 1986 April 11	15. PAGE COUNT 36															
16. SUPPLEMENTARY NOTATION This research was partially sponsored by DNA under Subtask W99QMXWA, work unit 00010 and work unit title "Plasma Structure Evolution," and by ONR.																		
17. COSATI CODES <table border="1"><tr><th>FIELD</th><th>GROUP</th><th>SUB-GROUP</th></tr><tr><td></td><td></td><td>Auroral ionosphere;</td></tr><tr><td></td><td></td><td>Auroral density irregularities</td></tr><tr><td></td><td></td><td>Current convective instability</td></tr><tr><td></td><td></td><td>Nonlocal plasma theory</td></tr></table>		FIELD	GROUP	SUB-GROUP			Auroral ionosphere;			Auroral density irregularities			Current convective instability			Nonlocal plasma theory	18. SUBJECT TERMS (Continue on reverse if necessary and identify by block number) Auroral ionosphere; Auroral density irregularities Current convective instability Nonlocal plasma theory	
FIELD	GROUP	SUB-GROUP																
		Auroral ionosphere;																
		Auroral density irregularities																
		Current convective instability																
		Nonlocal plasma theory																
19. ABSTRACT (Continue on reverse if necessary and identify by block number) It has been suggested that the current convective instability may be responsible for the structuring, i.e., generation of density irregularities, of density enhancements (known as "blobs") in the auroral ionosphere. However, previous theories have neglected the finite extent of the "blob" along the geomagnetic field. In this paper we develop a non-local theory of the current convective instability which considers the finite extent of an ionospheric "blob" parallel to the geomagnetic field. We find that the growth rate of the instability can be substantially reduced in the finite-sized "blob" case from the value obtained in the local approximation for an infinitely long blob. For auroral ionosphere parameters, the reduction in the growth rate for medium scale irregularities (1-10 km) can be one to two orders of magnitude for the typical observed values of "blob" sizes (~ a few hundred km). Thus, it appears that the current convective instability is not a viable mechanism to generate scintillation causing irregularities, i.e., 1-10 km irregularities.																		
20. DISTRIBUTION/AVAILABILITY OF ABSTRACT <input checked="" type="checkbox"/> UNCLASSIFIED/UNLIMITED <input type="checkbox"/> SAME AS RPT. <input type="checkbox"/> DTIC USERS		21. ABSTRACT SECURITY CLASSIFICATION UNCLASSIFIED																
22a. NAME OF RESPONSIBLE INDIVIDUAL J. D. Huba		22b. TELEPHONE (Include Area Code) (202) 767-3630	22c. OFFICE SYMBOL Code 4780															

CONTENTS

I. INTRODUCTION	1
II. MODEL AND FUNDAMENTAL EQUATIONS	4
III. DISPERSION EQUATION	8
IV. ANALYTICAL AND NUMERICAL RESULTS	13
V. DISCUSSION	15
ACKNOWLEDGMENTS	17
REFERENCES	20



Accession For	
NTIS	CRA&I <input checked="" type="checkbox"/>
DTIC	TAB <input type="checkbox"/>
Unannounced <input type="checkbox"/>	
Justification	
By _____	
Distribution / _____	
Availability Codes	
Dist	Avail and/or Special
A-1	23

THE EFFECT OF FINITE "BLOB" SIZE ON THE CURRENT CONVECTIVE INSTABILITY IN THE AURORAL IONOSPHERE

I. INTRODUCTION

Ionospheric irregularities (or density fluctuations) cause scintillation of radio signals which has been observed during diffuse auroral situations [Fremouw et al., 1977; Rino et al., 1978; Rino and Owen, 1980]. The irregularities occur in regions of soft particle precipitation (which are confined in latitude) and horizontal plasma density gradients. At present, the emerging picture is that large-scale density enhancements (known as "blobs") are produced in the high latitude F region and are convected around the polar ionosphere; the sides of these "blobs" appear to be the regions of structure [Tsunoda and Vickrey, 1985]. There has been a considerable theoretical effort to understand these irregularities in terms of gradient driven fluid instabilities [Ossakow and Chaturvedi, 1979; Huba and Ossakow, 1980; Vickrey et al., 1980; Keskinen et al., 1980; Chaturvedi and Ossakow, 1981, 1983; Keskinen and Ossakow, 1983; Satyanarayana and Ossakow, 1983; Gary, 1984; Huba, 1984; Satyanarayana et al., 1985]. In particular, the current convective instability [Lehnert, 1958; Kadomtsev and Nedospasov, 1960] has been suggested as a generation mechanism of plasma irregularities in the high latitude ionosphere [Ossakow and Chaturvedi, 1979; Fejer and Kelley, 1980; Hamuise et al., 1981; Vickrey and Kelley, 1983]. This instability can be excited in a weakly collisional, magnetized plasma which contains a field-aligned current and a transverse density gradient. This configuration exists, at times, in the auroral ionosphere along the sides of density enhancements ("blobs").

Manuscript approved December 6, 1985.

The theoretical study of the current convective instability, as applied to the auroral F region, has evolved over the years. Initial studies used the local approximation which is valid for modes such that $kL \gg 1$ where k is the wavenumber and L is the scale length of the density gradient [Ossakow and Chaturvedi, 1979; Vickrey et al., 1980; Chaturvedi and Ossakow, 1981; Gary, 1984]. Subsequent studies have considered a host of nonlocal effects which can be important and are neglected in a local analysis, e.g., magnetic shear [Huba and Ossakow, 1980]; velocity shear [Satyanarayana and Ossakow, 1983]; long wavelength modes (i.e., $kL < 1$) [Huba, 1984]; finite current channel width [Satyanarayana et al., 1985]. Overall, these effects have a tendency to reduce the growth rate of the instability, with the exception of velocity shear which can stabilize short wavelength modes (those with $kL \gg 1$). Despite the modest reductions in growth rate the current convective instability has remained a viable mechanism to generate density irregularities with scale lengths 1-10 km.

A potentially important nonlocal effect that has not been considered to date is the finite extent of the "blob" along the ambient geomagnetic field. For example, recent studies of barium cloud dynamics have indicated that the parallel extent of the cloud along the field can affect its stability properties [Goldman et al., 1976; Sperling et al., 1984; Sperling and Glassman, 1985; Drake et al., 1985]. Physically, the reason that this effect could be significant is the following. The current convective instability requires density and potential fluctuations both parallel and perpendicular to B_0 , i.e., assuming a Fourier expansion of the modes we have $\hat{k} = \hat{k}_\parallel + \hat{k}_\perp$ where \hat{k} is the wavenumber. Based on local theory, the instability attains maximum growth when $\hat{k}_\parallel / k_\perp = (\sigma_\parallel / \sigma_\perp)^{1/2}$ where σ_\parallel and σ_\perp are the plasma conductivities parallel and perpendicular to the

field, respectively. For typical F region parameters we note that $\sigma_1/\sigma_{\perp} = 10^8$ so that $\lambda_{\parallel} \sim 10^4 \lambda_{\perp}$ where λ is the wavelength of the mode. Thus, for fluctuations with $\lambda_{\perp} \sim 1-10$ km, local theory requires parallel wavelengths such that $\lambda_{\parallel} \sim 10^4 - 10^5$ km for maximum growth. On the other hand, the parallel extent of a "blob" is typically only several hundred km so that local theory is probably inadequate to properly describe the current convective instability in the auroral ionosphere (at least for the fastest growing modes of interest).

In this paper we develop a nonlocal theory of the current convective instability which considers the finite extent of an ionospheric "blob" parallel to the geomagnetic field. We show that the physical picture presented in the previous paragraph is, in fact, reasonably accurate. For a mode that has a parallel structure sufficiently short to "fit" the fastest growing mode into the "blob", we recover the maximum growth rate predicted by local theory. However, modes that have a parallel structure determined by the extent of the "blob" along the field can have growth rates substantially reduced from the maximum growth rate expected from local theory. For typical auroral ionosphere parameters, the reduction in the maximum growth rate of the instability for medium scale irregularities (1-10 km) can be one to two orders of magnitude.

The organization of the paper is as follows. In the next section we present the physical model and basic equations used in the analysis. In Section III we derive the dispersion equation for the current convective instability which explicitly includes the finite extent of the "blob" along the ambient magnetic field. In Section IV we present analytical and numerical results. Finally, in Section V we summarize our findings and apply our results to the auroral ionosphere.

II. MODEL AND FUNDAMENTAL EQUATIONS

We consider a slab geometry and a plasma configuration as shown in Fig. 1. The ambient magnetic field and current are in the z -direction ($\underline{B} = B_0 \hat{e}_z$ and $\underline{j} = J_0 \hat{e}_z$). The ambient density profile used is given by

$$n_0(x, z) = \begin{cases} n_b(x) & 0 < z < z_0 \\ n_i & \text{otherwise} \end{cases} \quad (1)$$

where n_b denotes the "blob" density which is confined to a limited region along B_0 and is inhomogeneous transverse to B_0 , and n_i denotes the homogeneous background ionosphere. We consider low frequency fluctuations such that $\partial/\partial t \ll \Omega_\alpha, v_{an}$ where Ω_α and v_{an} represent the gyrofrequency and collision frequency with neutrals associated with the α species. We also assume $v_{en}/\Omega_e \ll v_{in}/\Omega_i \ll 1$ which is relevant to the F region of the ionosphere. Finally, for simplicity we assume a cold plasma (i.e., $T_e = T_i = 0$) and that the ambient current is carried by electrons (i.e., $J_0 = -n_e v_{0z} \hat{e}_z$).

Within the context of our assumptions, the basic equations of our analysis are continuity, momentum transfer, charge neutrality, and Ampere's law:

$$\frac{\partial n_\alpha}{\partial t} + \nabla \cdot (n_\alpha \underline{v}_\alpha) = 0 \quad (2)$$

$$0 = -e\underline{E} - \frac{e}{c} \underline{v}_e \times \underline{B} - m_e v_{en} \underline{v}_e \quad (3)$$

$$0 = e\underline{E} + \frac{e}{c} \underline{v}_i \times \underline{B} - m_i v_{in} \underline{v}_i \quad (4)$$

$$\nabla \cdot \underline{J} = \nabla \cdot [ne(v_i - v_e)] = 0 \quad (5)$$

$$\nabla \times \underline{B} = \frac{4\pi}{c} \underline{J} \quad (6)$$

where the variables have their usual meanings and we are in the neutral frame of reference (i.e., $v_n = 0$). We take the electric and magnetic fields to be represented by potentials as

$$\underline{E} = -\nabla\phi - \frac{1}{c} \frac{\partial A_z}{\partial t} \hat{e}_z \quad (7)$$

and

$$\underline{B} = B_0 \hat{e}_z + \nabla A_z \times \hat{e}_z \quad (8)$$

where B_0 is the ambient field, and ϕ and A_z are the electrostatic and vector potentials, respectively. We consider only A_z since $J \gg J_{\perp}$.

The electron cross-field motion is given by

$$v_{e\perp} = -\frac{c}{B} \nabla_{\perp} \phi \times \hat{e}_z \quad (9)$$

while the parallel motion is given by

$$v_{e\parallel} = \frac{e}{m_e v_{en}} [\nabla_{\parallel} \phi + \frac{1}{c} \frac{\partial A_z}{\partial t}] \quad (10)$$

The ion cross-field motion is given by

$$v_{i\perp} = - \frac{c}{B} \nabla_{\perp} \phi \times \hat{e}_z - \frac{v_{in}}{\Omega_i} \frac{c}{B} \nabla_{\perp} \phi \quad (11)$$

and the parallel motion is given by

$$v_{i\parallel} = - \frac{m_e}{m_i} \frac{v_{en}}{v_{in}} v_{e\parallel} \ll v_{e\parallel}. \quad (12)$$

We now substitute (9)-(12) into (2), (5), and (6) and arrive at the following equations:

$$\frac{\partial n}{\partial t} + \frac{c}{B} \nabla_{\perp} \phi \times \hat{e}_z \cdot \nabla n + \frac{1}{4\pi e} \frac{\partial}{\partial z} \nabla_{\perp}^2 A_z = 0 \quad (13)$$

$$\frac{v_{in}}{\Omega_i} \frac{c}{B} \nabla \cdot (n \nabla_{\perp} \phi) + \frac{c}{4\pi e} \frac{\partial}{\partial z} \nabla_{\perp}^2 A_z = 0 \quad (14)$$

$$\nabla_{\perp}^2 A_z = \frac{4\pi}{cn_e} \frac{\partial \phi}{\partial z} + \frac{1}{c} \frac{\partial A_z}{\partial t} \quad (15)$$

where $n_e = m_e v_{en} / ne^2$.

The equilibrium solution of (13)-(15) requires that

$$- \frac{c}{B} \nabla_{\perp} \phi_0 \times \hat{e}_z \cdot \nabla n_0 + \frac{c}{4\pi e} \frac{\partial}{\partial z} \nabla_{\perp}^2 A_{z0} = 0 \quad (16)$$

$$\frac{v_{in}}{\Omega_i} \frac{c}{B} \nabla \cdot (n_0 \nabla_{\perp} \phi_0) + \frac{c}{4\pi e} \frac{\partial}{\partial z} \nabla_{\perp}^2 A_{z0} = 0 \quad (17)$$

$$\nabla_{\perp}^2 A_{z0} = \frac{4\pi}{cn_e} \frac{\partial \phi_0}{\partial z} \quad (18)$$

We have assumed $n_0 = n_0(x, z)$ [see (1)] and will also take ϕ_0 and A_{z0} to be functions only of x and z . [Neglect of the y dependence on ϕ_0 is equivalent to assuming $E_{0y} = 0$; we note that it is the y component

of E_0 which can drive the usual $E \times B$ gradient drift instability in the F region and we are excluding this possibility.] From (16) and (17) we then find that

$$\frac{c}{4\pi e} \frac{\partial}{\partial z} \nabla_{\perp}^2 A_{z0} = 0 \quad (19)$$

and

$$\frac{v_{in}}{\Omega_i} \frac{c}{B} \frac{\partial}{\partial x} (n_0 \nabla_{\perp} \phi_0) = 0 \quad (20)$$

Substituting (18) into (19) we find that

$$\frac{\partial}{\partial z} \frac{4\pi}{en_e} \frac{\partial \phi_0}{\partial z} = 0 \quad (21)$$

Making use of the definition of n_e ($= m_e v_{en} / ne^2$) and using (20) and (21) we can rewrite (14) as

$$\frac{v_{in}}{\Omega_i} \frac{\partial}{\partial x} (n_0 \frac{\partial \phi_0}{\partial x}) + \frac{\partial}{\partial z} \left(\frac{\Omega_e}{v_{en}} n_0 \frac{\partial \phi_0}{\partial z} \right) = 0 \quad (22)$$

which is equivalent to the requirement that $\nabla \cdot J_0 = 0$ since $J_{0x} = -n_0 (v_{in}/\Omega_i)(c/B)\partial \phi_0/\partial x$ and $J_{0z} = (n_0 e/m_e v_{en})\partial \phi_0/\partial z$.

Finally, we can write an equilibrium potential to be

$$\begin{aligned} \phi_0(x, z) &= -E_{0z} z - E_{0x} \int_z^x \frac{n_1 dx'}{n_b(x')} \quad 0 < z < z_0 \\ &= -E'_{0z} z \quad \text{otherwise} \end{aligned} \quad (23)$$

This potential generates an equilibrium electric field

$$\begin{aligned} \mathbf{E} = & E_{0z} \hat{\mathbf{e}}_z + E_{0x} n_i / n_b(x) \hat{\mathbf{e}}_x & 0 < z < z_0 \\ & E'_{0z} \hat{\mathbf{e}}_z & \text{otherwise} \end{aligned} \quad (24)$$

which causes a parallel electron drift $v_{0z} = - (eE_{0z}/m_e v_{en}) \hat{\mathbf{e}}_z$ and an inhomogeneous cross-field drift $v_{0\perp}(x) = - (cE_{0x}/B)(n_i/n_b(x)) \hat{\mathbf{e}}_y$ in the "blob" plasma. In the background plasma there is only a parallel electron drift $v'_{0z} = - (eE'_{0z}/m_e v_{en}) \hat{\mathbf{e}}_z$.

III. DISPERSION EQUATION

We linearize (13)-(15) in order to obtain the dispersion equation which describes the current convective instability. We use the equilibrium derived in Section II and assume perturbed quantities vary as $\tilde{p} = \tilde{p}(x) \exp(i\gamma t - ik_y y)$. The linearized equations are

$$\frac{\partial \tilde{n}}{\partial t} - \frac{c}{B} \nabla_{\perp} \tilde{\phi} \times \hat{\mathbf{e}}_z \cdot \nabla_{\perp} \tilde{n}_0 - \frac{c}{B} \nabla_{\perp} \tilde{\phi}_0 \times \hat{\mathbf{e}}_z \cdot \nabla \tilde{n} + \frac{c}{4\pi e} \frac{\partial}{\partial z} \nabla_{\perp}^2 \tilde{A}_z = 0 \quad (25)$$

$$\frac{v_{in}}{n_i} \frac{c}{B} \nabla \cdot (\tilde{n}_0 \nabla_{\perp} \tilde{\phi}) + \frac{v_{in}}{n_i} \frac{c}{B} \nabla \cdot (\tilde{n} \nabla_{\perp} \tilde{\phi}_0) + \frac{c}{4\pi e} \frac{\partial}{\partial z} \nabla_{\perp}^2 \tilde{A}_z = 0 \quad (26)$$

and

$$\nabla_{\perp}^2 \tilde{A}_z = \frac{4\pi e}{c} \tilde{n} V_{0z} + \frac{4\pi}{cn_e} \frac{\partial \tilde{\phi}}{\partial z} + \frac{1}{c} \frac{\partial \tilde{A}_z}{\partial t}. \quad (27)$$

In the following we will ignore terms proportional to $\nabla_{\perp} \tilde{\phi}_0$ which is valid for $k_y V_{0\perp} \ll |V_{0z} \partial/\partial z|$. Retaining these terms leads to two effects: (1)

a real frequency is produced proportional to $k_y V_{0\perp}(x_0)$ where $x = x_0$ is the location of mode localization, and (2) velocity shear stabilization of short wavelength modes (Satyanarayana and Ossakow, 1983). We are intentionally ignoring these effects in order to highlight the influence of finite "blob" size on the current convective instability.

Eliminating \bar{n} from these equations we obtain two coupled differential equations for \bar{A}_z and $\bar{\phi}$,

$$[\gamma + k_y^2 D_r] \bar{A}_z = -c \frac{\partial \bar{\phi}}{\partial z} + i \frac{\gamma_0}{\gamma \sqrt{a}} c k_y \bar{\phi} \quad (28)$$

and

$$\bar{\phi} = -\alpha D_r \frac{1}{c} \frac{\partial \bar{A}_z}{\partial z} \quad (29)$$

where $D_r = (c^2/\omega_{pe}^2)v_e$ is the resistive diffusion coefficient, $\omega_{pe}^2 = 4\pi n_0 e^2/m_e$, $\alpha = (\Omega_e/v_e)(\Omega_i/v_{in})$, and $\gamma_0 = -(v_e/\Omega_e)\sqrt{a} V_{0z} \partial \ln n_0 / \partial x$. In writing (28) we have taken $(V_{0z}/\gamma) \partial / \partial z \ll 1$ which can be shown a posteriori; this term does not affect the growth rate of the mode but only causes the mode to have a real frequency. Finally, combining (28) and (29), we obtain the mode equation for the current convective instability in terms of the vector potential \bar{A}_z ,

$$\frac{\partial}{\partial z} \left(\alpha D_r \frac{\partial A_z}{\partial z} \right) - i \frac{\gamma_0}{\gamma} \sqrt{a} D_r k_y \frac{\partial A_z}{\partial z} - (\gamma + k_y^2 D_r) A_z = 0. \quad (30)$$

Prior to solving (30) for the density profile shown in Fig. 1b, we first consider a blob of infinite extent along the field. We Fourier expand modes parallel to B_0 , i.e., $\tilde{p}(z) = \tilde{p} \exp(i k_z z)$ and use the local approximation [$k_y(\partial \ln n_0 / \partial x)^{-1} \gg 1$] so that (30) can be solved

algebraically. This allows comparison with previous results [Ossakow and Chaturvedi, 1979; Chaturvedi and Ossakow, 1981]. The local dispersion equation is given by

$$\gamma - \frac{\gamma_0}{\gamma} k_y k_z \sqrt{\alpha} D_r + (k_y^2 + \alpha k_z^2) D_r = 0. \quad (31)$$

The first term in (31) is related to electromagnetic effects, the second term to convection along the gradient (which causes the instability), and the final term to perpendicular ion motion and parallel electron motion. In the electrostatic limit ($k_y^2 D_r, \alpha k_z^2 D_r \gg \gamma$) the growth rate is given by

$$\gamma = + \gamma_0 \frac{\sqrt{\alpha} (k_z/k_y)}{1 + \alpha k_z^2/k_y^2} \quad (32)$$

which agrees with the results of Ossakow and Chaturvedi (1979). This growth rate has a maximum value when $k_z^2/k_y^2 = 1/\alpha$. It is given by

$$\gamma_{\max} = \gamma_0/2 \quad (33)$$

Retention of electromagnetic effects yields the following growth rate

$$\gamma = - \frac{1}{2} \hat{k}^2 D_r \pm \frac{1}{2} [\hat{k}^2 D_r + 4\gamma_0 k_y k_z \sqrt{\alpha} D_r]^{1/2} \quad (34)$$

where $\hat{k}^2 = k_y^2 + \alpha k_z^2$ and which can be shown to agree with Chaturvedi and Ossakow (1981).

We now solve (30) for a density profile relevant to a plasma "blob" in the auroral ionosphere. The equation is solved subject to the boundary

condition $\tilde{A}_z \rightarrow 0$ as $|z| \rightarrow \infty$. For a "top hat" density profile (Fig. 1b), the solution to (30) in the region $z < 0$ and $z > z_0$ can be written as a plane wave,

$$\tilde{A}_z = \tilde{A}_i \exp(-k_i |z|) \quad (35)$$

where

$$k_i = k_y \left(\frac{1}{\sqrt{\alpha R}} \right) \quad (36)$$

and

$$R = \frac{k_y^2 D_r}{\gamma + k_y^2 D_r} \quad (37)$$

Note that the subscript i denotes quantities that are evaluated in the background ionosphere (i.e., $z < 0$ and $z > z_0$). The parameter R is a measure of the electrostatic/electromagnetic nature of the mode. For $\gamma \ll k_y^2 D_r$ we note that $R \approx 1$ and the mode is essentially electrostatic. In the opposite limit, $\gamma \gg k_y^2 D_r$ the mode is essentially electromagnetic with $R \ll 1$.

In the region $0 < z < z_0$, i.e., region occupied by the density enhancement, the solution to \tilde{A}_z is given by

$$\tilde{A}_z = \tilde{A}_{zb}^1 \exp(ik_1 z) + \tilde{A}_{zb}^2 \exp(ik_2 z) \quad (38)$$

where

$$k_1 = \frac{k_y}{\sqrt{\alpha}} \left[-\frac{1}{2} \frac{\gamma_0}{\gamma} + \frac{1}{2} \left(\frac{\gamma_0^2}{\gamma^2} - \frac{4}{R} \right)^{1/2} \right]_b \quad (39)$$

and

$$k_2 = \frac{k_y}{\sqrt{\alpha}} \left[-\frac{1}{2} \frac{\gamma_0}{\gamma} - \frac{1}{2} \left(\frac{\gamma_0^2}{\gamma^2} - \frac{4}{R} \right)^{1/2} \right]_b \quad (40)$$

Again, the subscript b denotes quantities that are to be evaluated in the blob ($0 < z < z_0$).

To determine the dispersion equation we match the plane wave solutions at $z = 0$ and $z = z_0$. The appropriate matching conditions are obtained from (28) and (29). Namely, we require that \hat{A}_z and $\alpha D_r \partial A_z / \partial z$ be continuous across each boundary. Using these boundary conditions, we find that the dispersion equation is given by

$$\exp(i\Delta kz_0) = \Lambda \quad (41)$$

where

$$\Lambda = \frac{1 + i\Gamma \frac{k_2}{k_1}}{1 + i\Gamma \frac{k_1}{k_1}} \frac{1 - i\Gamma \frac{k_1}{k_1}}{1 - i\Gamma \frac{k_2}{k_1}} \quad (42)$$

$$\Delta k = k_1 - k_2 = \frac{k_y}{\sqrt{\alpha}} \left[\frac{\gamma_0^2}{\gamma^2} - \frac{4}{R} \right]_b^{1/2} \quad (43)$$

$$\Gamma = \frac{(\alpha D_r)_b}{(\alpha D_r)_i} \quad (44)$$

and k_1 , k_1 , and k_2 are given in (36), (39), and (40), respectively.

IV. ANALYTICAL AND NUMERICAL RESULTS

We now present analytical and numerical results for the growth rate of the current convective instability based upon (41). We cast (41) into dimensionless form and obtain

$$\exp(i\hat{k}_y \hat{z}_0 \hat{\Delta k}) = \Lambda \quad (45)$$

where $\hat{k}_y = k_y L_r$, $\hat{z}_0 = z_0 / \sqrt{\alpha} L_r$, $\hat{\Delta k} = \Delta k / k_y$, and $L_r = D_r / Y_0$ is the resistive diffusion length. First, we note that in the short wavelength limit, i.e., when $\hat{k}_y \hat{z}_0 \gg 1$, $k_1 = k_2$ which implies $\hat{\Delta k} = 0$, so that $\Lambda = 1$ is a solution to (45). The growth rate is given by

$$\gamma = \frac{Y_0}{2} \sqrt{R_b}. \quad (46)$$

In the electrostatic limit ($\gamma \ll k_y^2 D_r$) we note that $R = 1$ and $Y = Y_0/2$ which corresponds to the maximum growth rate of the instability based upon local theory [see (33)]. This result makes sense physically since the limit $\hat{k}_y \hat{z}_0 \gg 1$ corresponds to modes with parallel wavelengths much smaller than the parallel length of the blob; hence, the outer regions (i.e., $z < 0$ and $z > z_0$) have little affect on the dynamics of the instability.

On the other hand, for long wavelengths, i.e., $\hat{k}_y \hat{z}_0 \ll 1$, the growth rate is strongly affected by the finite length of the blob. The growth rate is reduced and $k_2 \gg k_1$. In this limit $\Lambda = -1$ and the dispersion equation becomes

$$\hat{k}_y \hat{z}_0 \hat{\Delta k} = (2m + 1)\pi \quad (47)$$

where $m = 1, 2, \dots$ is an integer. Equation (47) yields the following growth rate

$$\gamma = \gamma_0 \frac{\hat{k}_y z_0}{(2m + 1)\pi} \quad (48)$$

We note that this growth rate is independent of the value of R . Also, the fastest growing mode in this regime corresponds to $m = 0$.

In Fig. 2 we present numerical results based upon (45). We plot $\hat{\gamma} = \gamma/\gamma_0$ versus $\hat{k}_y = k_y L_r$ for $\hat{z}_0 = z_0/\sqrt{a} L_r = 1$ and $\Gamma = 0.2$ for several values of mode number m . The solid curves are numerical results while the dashed curves are based upon the analytical results (46) and (48). Note the excellent agreement between these results in the short wavelength (i.e., $\hat{k}_y \gg 2\pi$) and long wavelength (i.e., $\hat{k}_y \ll 2\pi$) limits. In the short wavelength regime the modes are electrostatic ($R \sim 1$) and have a growth rate which is the same as the maximum value obtained from local theory [$\gamma = \gamma_0/2$, see (33)]. In the long wavelength limit the modes are electromagnetic ($R \ll 1$) and have a smaller growth rate than in the short wavelength limit.

Physically, the reduction in growth can be explained as follows. The current convective instability requires a density and potential perturbation parallel to B_0 which corresponds to a parallel wavenumber in the local analysis (the second term in (31) is the driver and depends upon γ_0 and k_z). From local theory, the instability achieves maximum growth when $k_z/k_y = 1/\sqrt{a} = (\sigma_{\perp}/\sigma_{\parallel})^{1/2}$ where σ_{\perp} and σ_{\parallel} are the perpendicular and parallel conductivities, respectively. In the ionosphere, $\sigma_{\perp}/\sigma_{\parallel} - 10^{-8} \ll 1$ so that the instability favors very long wavelengths parallel

to B_0 relative to the perpendicular wavelengths ($\lambda_{\parallel} \gg \lambda_{\perp}$). We define the maximum effective parallel wavenumber that can be supported within the blob as

$$k_{z(\text{eff})} = 2\pi/z_0. \quad (49)$$

Using (49) to determine the value of $\hat{k}_y \hat{z}_0$ for maximum growth based on local theory ($k_y/k_z = \sqrt{\alpha}$) we find that $\hat{k}_y \hat{z}_0 = 2\pi$. Thus, for $\hat{k}_y \hat{z}_0 \gg 2\pi$ we expect that the blob is sufficiently long to support a parallel wavelength which yields maximum growth, i.e., $k_z > k_{z(\text{eff})}$. This is, in fact, quite apparent in Fig. 2 where $\gamma = 0.5$ for $\hat{k}_y \hat{z}_0 \gg 2\pi$. However, for modes such that $\hat{k}_y \hat{z}_0 \ll 2\pi$ it is not possible for any mode to satisfy the condition $k_z/k_y = 1/\sqrt{\alpha}$. Therefore, the modes grow at a reduced growth rate; again this is apparent from Fig. 2. In fact, this corresponds to the limit $\sqrt{\alpha} k_z/k_y \gg 1$ based on local theory. Making use of this approximation in (32) we find that

$$\gamma = \gamma_0 \frac{k_y}{\sqrt{\alpha} k_z} \quad (50)$$

which agrees with (48) if we make the identification $k_z^{-1} = z_0/(2m + 1)\pi$.

V. DISCUSSION

We have studied the effects of finite size of high latitude "blobs" parallel to magnetic field on the current convective instability in auroral ionosphere. We find that the growth rate of the instability can be substantially reduced in the case of a finite size "blob" from the value obtained when the "blobs" are assumed to be infinite. For short

wavelengths, such that $k_y z_0 \gg \sqrt{\alpha}$ (where k is the wavenumber, z_0 the blob size and $\alpha = \Omega_e \Omega_i / v_{e\perp} v_{i\perp} = \sigma_\parallel / \sigma_\perp$), the growth rate remains relatively unaffected (especially in the electrostatic case) by the blob size. In the long wavelength case, when $k_y z_0 \ll \sqrt{\alpha}$, the growth rate becomes proportional to the wavenumber and the blob size. Thus, for a given blob size, the longer transverse wavelengths have smaller growth rates and, similarly, for shorter blob sizes, the growth rates are reduced [see (48)].

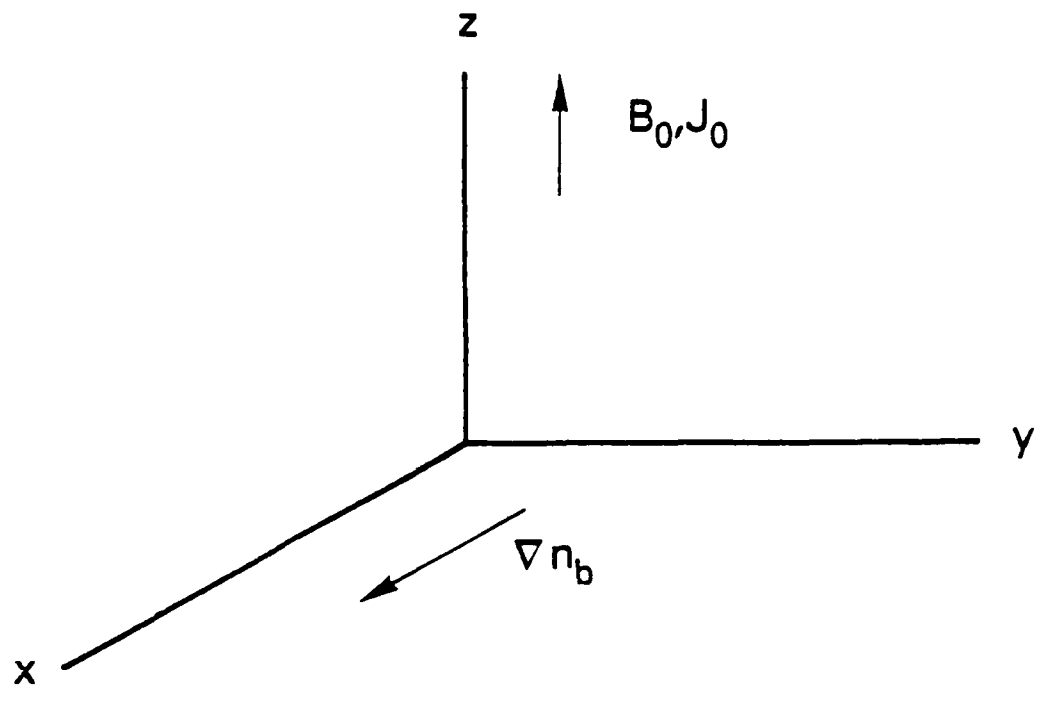
The current convective instability has been discussed in the auroral ionosphere recently, where field-aligned currents are a constant feature and plasma density enhancements ("blobs") have been observed with structured walls. We now apply our results for the instability to this situation. The typical parameters in this situation are the following: ambient density $n_i = 10^6 \text{ cm}^{-3}$, blob density $n_b = 5 \times 10^6 \text{ cm}^{-3}$, field-aligned current density $J_{\parallel 0} \leq 10^2 \text{ amp/m}^2$ (which corresponds to an electron parallel drift $v_{0\parallel} \leq 300 \text{ m/sec}$ for $n_b = 10^6 \text{ cm}^{-3}$), the scale length associated with the "blob" gradient $L_N = 50 \text{ kms}$, the ion-neutral collision frequency $\nu_{in} = 5 \times 10^{-2} \text{ sec}^{-1}$ and electron collision frequency $\nu_e = 5 \times 10^2 \text{ sec}^{-1}$ [Tsunoda and Vickrey, 1985]. For $B_0 = 0.5 \text{ G}$, one has $\nu_e/\Omega_e = 6 \times 10^{-5}$ and $\nu_{in}/\Omega_i = 1.7 \times 10^{-4}$ so that $\alpha = (\Omega_e \Omega_i / v_{e\perp} v_{i\perp}) = 10^3$. The maximum local growth rate is $\gamma_m = \gamma_0/2 = 3.5 \times 10^{-3} \text{ sec}^{-1}$, where $\gamma_0 = (v_{0\parallel}/L_N)(\Omega_e v_i / v_e \Omega_i) = 1.7 \times 10^{-2} \text{ sec}^{-1}$. The "blob" dimension parallel to the field is $z_0 = 300 \text{ km}$ [Tsunoda and Vickrey, 1985] and for the above set of parameters we have $\omega_{pe} = 5.6 \times 10^7 \text{ sec}^{-1}$, $D_{ri} = 1.4 \times 10^8 \text{ cm}^2/\text{sec}$, $L_r = D_{ri}/\gamma_0 = 3 \times 10^9 \text{ cm}$, and $\hat{z}_0 = z_0/\sqrt{\alpha} L_r = 3.8 \times 10^{-7}$. For $\lambda_\perp = 1 \text{ km}$, $\hat{k}_y = k_y L_r = 5 \times 10^5$, and $\hat{k}_y \hat{z}_0 = 0.2$. We find from (48), that the nonlocal growth rate in this instance is $\gamma = 0.06 \gamma_0 = 1.0 \times 10^{-3} \text{ sec}^{-1}$ for the fastest growing mode ($m = 0$). This is an order of magnitude smaller

than the maximum local growth γ_m , i.e., $\gamma_m = 8.5 \times 10^{-3} \text{ sec}^{-1}$. For a similar set of parameters, we find that for $\lambda_{\perp} \sim 10 \text{ km}$, the reduction in the growth rate is even more substantial, i.e., $\gamma = 0.006 \gamma_0 = 1.0 \times 10^{-4} \text{ sec}^{-1}$. Therefore, the current convective instability growth rates may be too small for the instability to explain the blob-associated structure for irregularity scale-sizes of $1 - 10 \text{ km}$.

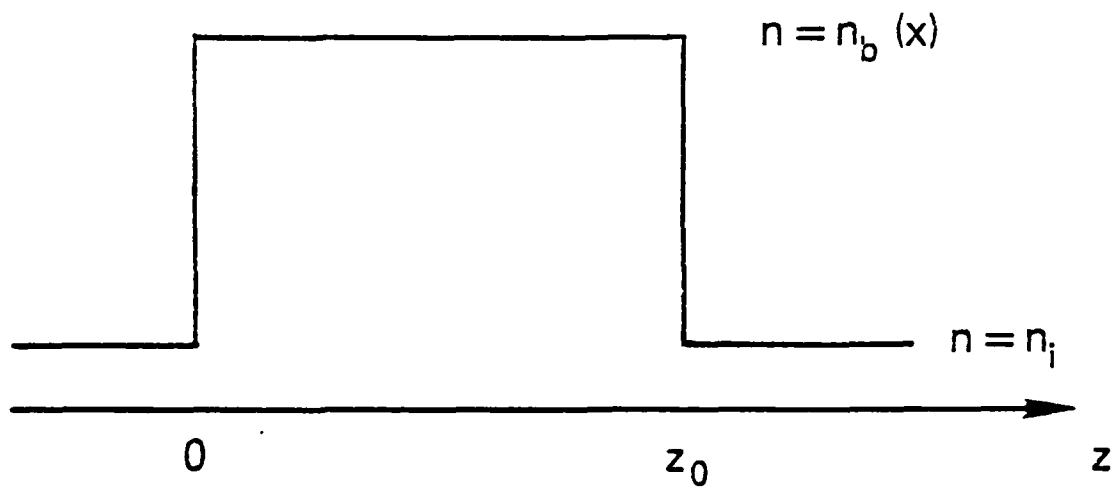
It may be pointed out that the finite blob-size induced reduction in the current convective instability growth rate of the instability is also related to our assumption that the instability region is confined to the "blob" (i.e., the driving density gradient is negligible outside the blob, namely, in the ambient ionosphere). This is represented by the requirement that the modes decay exponentially outside the blob. This is a reasonable assumption in the blob-associated structure studies. However, should there be a transverse gradient in the ambient ionosphere at high altitude F-region, and if a positive correlation is observed between the structure and the field-aligned currents, then the current convective instability could be considered a possible mechanism for scale sizes on the order of a few km or less.

ACKNOWLEDGMENTS

We thank Drs. J. Drake and M. Keskinen for beneficial discussions. We thank one of the referees for comments that led to improvements in our equilibrium model. This research was supported by the Defense Nuclear Agency and the Office of Naval Research.



(a)



(b)

Fig. 1) Plasma configuration and slab geometry. (a) Coordinate system and ambient plasma properties. (b) "Top hat" density model for plasma along the ambient magnetic field.

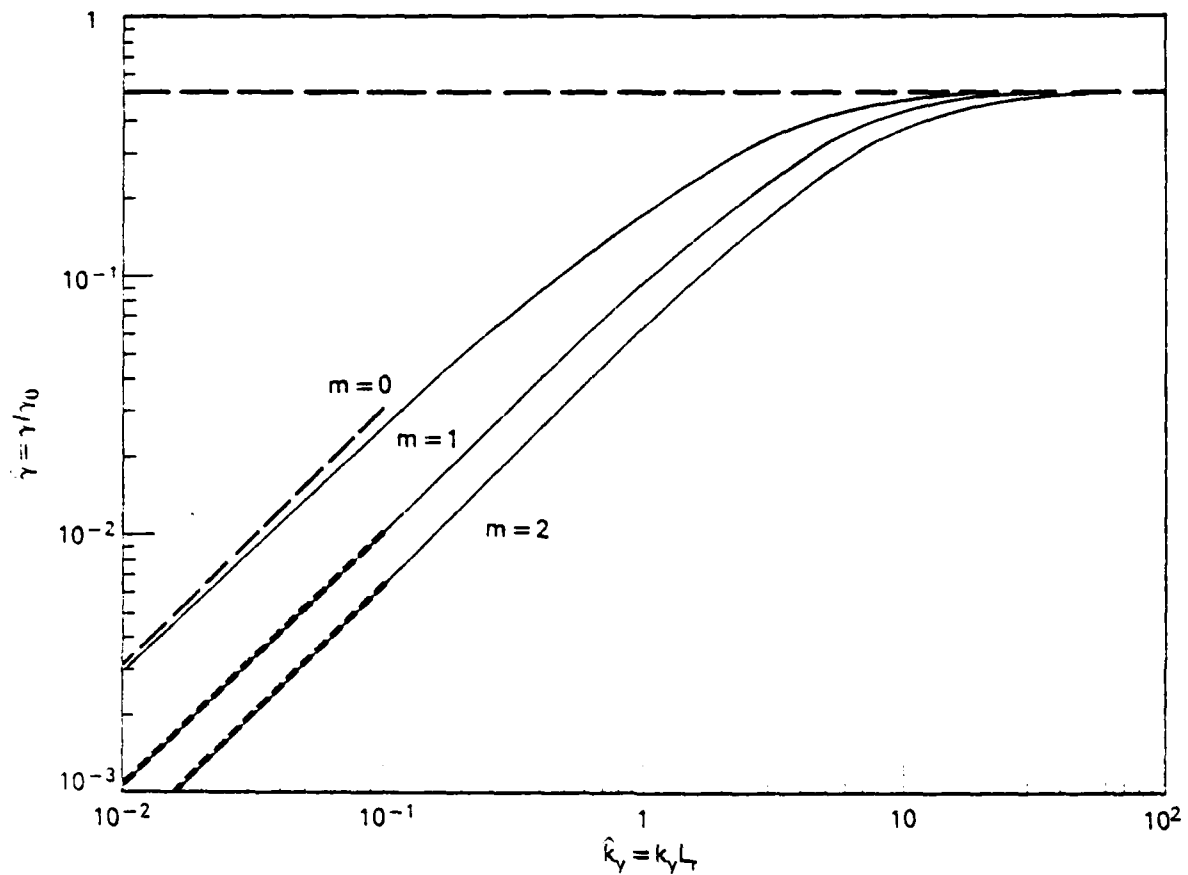


Fig. 2) Plot of growth rate ($\hat{Y} = \gamma/\gamma_0$) versus perpendicular wavenumber ($\hat{k}_y = k_y L_r$) for several mode numbers ($m = 0, 1, 2$). The solid curves are numerical solutions of the dispersion equation (45) while the dashed curves are analytic solutions. For $\hat{k}_y \gg 1$ we use (46) while for $\hat{k}_y \ll 1$ we use (48).

REFERENCES

- Chaturvedi, P.K. and S.L. Ossakow, The current convective instability as applied to the auroral ionosphere, J. Geophys. Res., 86, 4811, 1981.
- Chaturvedi, P.K. and S.L. Ossakow, Effect of an electron beam on the current convective instability, J. Geophys. Res., 88, 4114, 1983.
- Drake, J.F., J.D. Huba, and S.T. Zalesak, Finite temperature stabilization of the gradient drift instability in barium clouds, J. Geophys. Res., 90, 5227, 1985.
- Fejer, B.G. and M.C. Kelley, Ionospheric irregularities, Rev. Geophys. Space Phys., 18, 401, 1980.
- Fremouw, E.J., C.L. Rino, R.C. Livingston, and M.C. Cousins, A persistent subauroral scintillation enhancement observed in Alaska, Geophys. Res. Lett., 4, 539, 1977.
- Gary, S.P., Kinetic theory of current and density drift instabilities with weak charged-neutral collisions, J. Geophys. Res., 89, 179, 1984.
- Goldman, S.R., L. Baker, S. Ossakow, and A.J. Scannapieco, Striation formation associated with barium clouds in an inhomogeneous ionosphere, J. Geophys. Res., 81, 5097, 1976.
- Hanuise, C., J.P. Villain and M. Crochet, Spectral studies of F region irregularities in the auroral zone, Geophys. Res. Lett., 8, 1083, 1981.
- Huba, J.D. and S.L. Ossakow, Influence of magnetic shear on the current convective instability in the diffuse aurora, J. Geophys. Res., 85, 6874, 1980.
- Huba, J.D., Long wavelength limit of the current convective instability, J. Geophys. Res., 89, 2931, 1984.

- Kadomtsev, S.B. and A.V. Nedospasov, Instability of the positive column in a magnetic field and the "anomalous diffusion effect", *J. Nucl. Energy, Part C, Plasma Physics*, 1, 230, 1960.
- Keskinen, M.J., S.L. Ossakow, and B.E. McDonald, Nonlinear evolution of diffuse auroral F region ionospheric irregularities, *Geophys. Res. Lett.*, 7, 573, 1980.
- Keskinen, M.J. and S.L. Ossakow, Theories of high latitude ionospheric irregularities: A review, *Radio Sci.*, 18, 1077, 1983.
- Lehnert, B., Diffusion processes in the positive column in a longitudinal magnetic field, in Proceedings of the Second Geneva Conference on the Peaceful Uses of Atomic Energy, 32, 349, 1958.
- Ossakow, S.L. and P.K. Chaturvedi, Current convective instability in the diffuse aurora, *Geophys. Res. Lett.*, 6, 332, 1979.
- Rino, C.L., R.C. Livingston, and S.J. Mathews, Evidence for sheet-like auroral ionospheric irregularities, *Geophys. Res. Lett.*, 5, 1039, 1978.
- Rino, C.L. and J. Owen, The structure of localized nighttime auroral-zone scintillation enhancements, *J. Geophys. Res.*, 85, 2941, 1980.
- Satyana Rayana, P. and S.L. Ossakow, Influence of velocity shear on the current convective instability, *J. Geophys. Res.*, 89, 3019, 1983.
- Satyana Rayana, P., J. Chen, and M.J. Keskinen, Effects of finite current channel width on the current convective instability, *J. Geophys. Res.*, 90, 4311, 1985.
- Sperling, J.L., J.F. Drake, S.T. Zalesak, and J.D. Huba, The role of finite parallel length on the stability of barium clouds, *J. Geophys. Res.*, 89, 10913, 1984.

Sperling, J.L. and A.J. Glassman, Striation eigenmodes along the geomagnetic field and eigenvalues in the limit of strong ion-neutral collisions, J. Geophys. Res., 90, 2819, 1985.

Tsunoda, R.T. and J.F. Vickrey, Evidence of east-west structure in large-scale F-region plasma enhancements in the auroral zone, submitted to the Journal of Geophysical Research, 1985.

Vickrey, J.F., C.L. Rino, and T.A. Potemra, Chatanika/TRIAD observations of unstable ionization enhancements in the auroral F region, Geophys. Res. Lett., 7, 789, 1980.

Vickrey, J.F. and M.C. Kelley, Irregularities and instabilities in the auroral F-region, High latitude space plasma physics, edited by B. Hultqvist and T. Hagfors, Plenum, New York, 1983.

DISTRIBUTION LIST

DEPARTMENT OF DEFENSE

ASSISTANT SECRETARY OF DEFENSE
COMM, CMD, CONT 7 INTELL
WASHINGTON, DC 20301

DIRECTOR
COMMAND CONTROL TECHNICAL CENTER
PENTAGON RM BE 685
WASHINGTON, DC 20301
O1CY ATTN C-650
O1CY ATTN C-312 R. MASON

DIRECTOR
DEFENSE ADVANCED RSCH PROJ AGENCY
ARCHITECT BUILDING
1400 WILSON BLVD.
ARLINGTON, VA 22209
O1CY ATTN NUCLEAR
MONITORING RESEARCH
O1CY ATTN STRATEGIC TECH OFFICE

DEFENSE COMMUNICATION ENGINEER CENTER
1860 WIEHLE AVENUE
RESTON, VA 22090
O1CY ATTN CODE R410
O1CY ATTN CODE R812

DIRECTOR
DEFENSE NUCLEAR AGENCY
WASHINGTON, DC 20305
O1CY ATTN STVL
O4CY ATTN TITL
O1CY ATTN DDST
O3CY ATTN RAAE

COMMANDER
FIELD COMMAND
DEFENSE NUCLEAR AGENCY
KIRTLAND, AFB, NM 87115
O1CY ATTN FCPR

DEFENSE NUCLEAR AGENCY
SAO/DNA
BUILDING 20676
KIRTLAND AFB, NM 87115
O1CY D.C. THORNBURG

DIRECTOR
INTERSERVICE NUCLEAR WEAPONS SCHOOL
KIRTLAND AFB, NM 87115
O1CY ATTN DOCUMENT CONTROL

JOINT PROGRAM MANAGEMENT OFFICE
WASHINGTON, DC 20330
O1CY ATTN J-3 WWMCCS EVALUATION
OFFICE

DIRECTOR
JOINT STRAT TGT PLANNING STAFF
OFFUTT AFB
OMAHA, NB 68113
O1CY ATTN JSTPS/JLKS
O1CY ATTN JPST G. GOETZ

CHIEF
LIVERMORE DIVISION FLD COMMAND DNA
DEPARTMENT OF DEFENSE
LAWRENCE LIVERMORE LABORATORY
P.O. BOX 808
LIVERMORE, CA 94550
O1CY ATTN FCPRL

COMMANDANT
NATO SCHOOL (SHAPE)
APO NEW YORK 09172
O1CY ATTN U.S. DOCUMENTS OFFICER

UNDER SECY OF DEF FOR RSCH & ENGRG
DEPARTMENT OF DEFENSE
WASHINGTON, DC 20301
O1CY ATTN STRATEGIC & SPACE
SYSTEMS (CS)

COMMANDER/DIRECTOR
ATMOSPHERIC SCIENCES LABORATORY
U.S. ARMY ELECTRONICS COMMAND
WHITE SANDS MISSILE RANGE, NM 88002
O1CY ATTN DELAS-EO, F. NILES

DIRECTOR
BMD ADVANCED TECH CTR
HUNTSVILLE OFFICE
P.O. BOX 1500
HUNTSVILLE, AL 35807
01CY ATTN ATC-T MELVIN T. CAPPS
01CY ATTN ATC-O W. DAVIES
01CY ATTN ATC-R DON RUSS

PROGRAM MANAGER
BMD PROGRAM OFFICE
5001 EISENHOWER AVENUE
ALEXANDRIA, VA 22333
01CY ATTN DACS-BMT J. SHEA

CHIEF C-E- SERVICES DIVISION
U.S. ARMY COMMUNICATIONS CMD
PENTAGON RM 1B269
WASHINGTON, DC 20310
01CY ATTN C- E-SERVICES DIVISION

COMMANDER
FRADCOM TECHNICAL SUPPORT ACTIVITY
DEPARTMENT OF THE ARMY
FORT MONMOUTH, N.J. 07703
01CY ATTN DRSEL-NL-RD H. BENNET
01CY ATTN DRSEL-PL-ENV H. BCMKE
01CY ATTN J.E. QUIGLEY

COMMANDER
U.S. ARMY COMM-ELEC ENGRG INSTAL AGY
FT. HUACHUCA, AZ 85613
01CY ATTN CCC-EMEO GEORGE LANE

COMMANDER
U.S. ARMY FOREIGN SCIENCE & TECH CTR
220 7TH STREET, NE
CHARLOTTESVILLE, VA 22901
01CY ATTN DRXST-SD

COMMANDER
U.S. ARMY MATERIAL DEV & READINESS CMD
5001 EISENHOWER AVENUE
ALEXANDRIA, VA 22333
01CY ATTN DRCLDC J.A. BENDER

COMMANDER
U.S. ARMY NUCLEAR AND CHEMICAL AGENCY
7500 BACKLICK ROAD
BLDG 2073
SPRINGFIELD, VA 22150
01CY ATTN LIBRARY

DIRECTOR
U.S. ARMY BALLISTIC RESEARCH
LABORATORY
ABERDEEN PROVING GROUND, MD 21005
01CY ATTN TECH LIBRARY,
EDWARD BAICY

COMMANDER
U.S. ARMY SATCOM AGENCY
FT. MONMOUTH, NJ 07703
01CY ATTN DOCUMENT CONTROL

COMMANDER
U.S. ARMY MISSILE INTELLIGENCE AGENCY
REDSTONE ARSENAL, AL 35809
01CY ATTN JIM GAMBLE

DIRECTOR
U.S. ARMY TRADOC SYSTEMS ANALYSIS
ACTIVITY
WHITE SANDS MISSILE RANGE, NM 88002
01CY ATTN ATAA-SA
01CY ATTN TCC/F. PAYAN JR.
01CY ATTN ATTA-TAC LTC J. HESSE

COMMANDER
NAVAL ELECTRONIC SYSTEMS COMMAND
WASHINGTON, DC 20360
01CY ATTN NAVALEX 034 T. HUGHES
01CY ATTN PME 117
01CY ATTN PME 117-T
01CY ATTN CODE 5011

COMMANDING OFFICER
NAVAL INTELLIGENCE SUPPORT CTR
4301 SUITLAND ROAD, BLDG. 5
WASHINGTON, DC 20330
01CY ATTN MR. DUBBIN STIC 12
01CY ATTN NISC-60
01CY ATTN CODE 5404 J. GALET

COMMANDER
NAVAL OCCEAN SYSTEMS CENTER
SAN DIEGO, CA 92152
01CY ATTN J. FERGUSON

NAVAL RESEARCH LABORATORY WASHINGTON, DC 20375	COMMANDER AEROSPACE DEFENSE COMMAND/DC DEPARTMENT OF THE AIR FORCE ENT AFB, CO 80912
01CY ATTN CODE 4700 S.L. Ossakow, 26 CYS IF UNCLASS (01CY IF CLASS)	01CY ATTN DC MR. LONG
ATTN CODE 4730 J.D. HUBA, 50 CYS IF UNCLASS, 01CY IF CLASS	
01CY ATTN CODE 4701 I. VITKOVITSKY	COMMANDER AEROSPACE DEFENSE COMMAND/XPD
01CY ATTN CODE 7500	DEPARTMENT OF THE AIR FORCE
01CY ATTN CODE 7550	ENT AFB, CO 80912
01CY ATTN CODE 7580	01CY ATTN XPDQQ
01CY ATTN CODE 7551	01CY ATTN XP
01CY ATTN CODE 7555	
01CY ATTN CODE 4730 E. MCLEAN	AIR FORCE GEOPHYSICS LABORATORY
01CY ATTN CODE 4108	HANSCOM AFB, MA 01731
01CY ATTN CODE 4730 B. RIPIN	01CY ATTN OPR HAROLD GARDNER
20CY ATTN CODE 2628	01CY ATTN LKB
COMMANDER NAVAL SPACE SURVEILLANCE SYSTEM DAHLGREN, VA 22448 01CY ATTN CAPT J.H. BURTON	KENNETH S.W. CHAMPION
OFFICER-IN-CHARGE NAVAL SURFACE WEAPONS CENTER WHITE OAK, SILVER SPRING, MD 20910 01CY ATTN CODE F31	01CY ATTN OPR ALVA T. STAIR
DIRECTOR STRATEGIC SYSTEMS PROJECT OFFICE DEPARTMENT OF THE NAVY WASHINGTON, DC 20375 01CY ATTN NSP-2141 01CY ATTN NSSP-2722 FRED WIMBERLY	01CY ATTN PHD JURGEN BUCHAU
COMMANDER NAVAL SURFACE WEAPONS CENTER DAHLGREN LABORATORY DAHLGREN, VA 22448 01CY ATTN CODE DF-14 R. BUTLER	01CY ATTN PHD JOHN P. MULLEN
OFFICER OF NAVAL RESEARCH ARLINGTON, VA 22217 01CY ATTN CODE 465 01CY ATTN CODE 461 01CY ATTN CODE 402 01CY ATTN CODE 420 01CY ATTN CODE 421	AF WEAPONS LABORATORY KIRTLAND AFT, NM 87117
	01CY ATTN SUL
	01CY ATTN CA ARTHUR H. GUENTHER
	01CY ATTN NTYCE 1LT. G. KRAJEI
	AFTAC PATRICK AFB, FL 32925
	01CY ATTN TN
	AIR FORCE AVIONICS LABORATORY WRIGHT-PATTERSON AFB, OH 45433
	01CY ATTN AAD WADE HUNT
	01CY ATTN AAD ALLEN JOHNSON
	DEPUTY CHIEF OF STAFF RESEARCH, DEVELOPMENT, & ACQ DEPARTMENT OF THE AIR FORCE WASHINGTON, DC 20330 01CY ATTN AFRDQQ
	HEADQUARTERS ELECTRONIC SYSTEMS DIVISION DEPARTMENT OF THE AIR FORCE HANSCOM AFB, MA 01731-5000 01CY ATTN J. DEAS ESD/SCD-4

COMMANDER
FOREIGN TECHNOLOGY DIVISION, AFSC
WRIGHT-PATTERSON AFB, OH 45433
O1CY ATTN NICD LIBRARY
O1CY ATTN STDP B. BALLARD

COMMANDER
ROME AIR DEVELOPMENT CENTER, AFSC
GRIFFISS AFB, NY 13441
O1CY ATTN DOC LIBRARY/TSLD
O1CY ATTN DCSE V. COYNE

STRATEGIC AIR COMMAND/XPFS
OFFUTT AFB, NB 68113
O1CY ATTN ADWATE MAJ BRUCE BAUER
O1CY ATTN NRT
O1CY ATTN DOK CHIEF SCIENTIST

SAMSO/SK
P.O. BOX 92960
WORLDWAY POSTAL CENTER
LOS ANGELES, CA 90009
O1CY ATTN SKA (SPACE COMM SYSTEMS)
M. CLAVIN

SAMSO/MN
NORTON AFB, CA 92409
(MINUTEMAN)
O1CY ATTN MNML

COMMANDER
ROME AIR DEVELOPMENT CENTER, AFSC
HANSOM AFB, MA 01731
O1CY ATTN EEP A. LORENTZEN

DEPARTMENT OF ENERGY
LIBRARY ROOM C-042
WASHINGTON, DC 20545
O1CY ATTN DOC CON FOR A. LABOWITZ

DEPARTMENT OF ENERGY
ALBUQUERQUE OPERATIONS OFFICE
P.O. BOX 5400
ALBUQUERQUE, NM 87115
O1CY ATTN DOC CON FOR D. SHERWOOD

EG&G, INC.
LOS ALAMOS DIVISION
P.O. BOX 809
LOS ALAMOS, NM 85544
O1CY ATTN DOC CON FOR J. BREEDLOVE

UNIVERSITY OF CALIFORNIA
LAWRENCE LIVERMORE LABORATORY
P.O. BOX 308
LIVERMORE, CA 94550
O1CY ATTN DOC CON FOR TECH INFO
DEPT
O1CY ATTN DOC CON FOR L-389 R. OTT
O1CY ATTN DOC CON FOR L-31 R. HAGE

LOS ALAMOS NATIONAL LABORATORY
P.O. BOX 1663
LOS ALAMOS, NM 87545
O1CY ATTN DOC CON FOR J. WOLCOTT
O1CY ATTN DOC CON FOR R.F. TASCHEK
O1CY ATTN DOC CON FOR E. JONES
O1CY ATTN DOC CON FOR J. MALIK
O1CY ATTN DOC CON FOR R. JEFFRIES
O1CY ATTN DOC CON FOR J. ZINN
O1CY ATTN DOC CON FOR D. WESTERVEL
O1CY ATTN D. SAPPENFIELD

LOS ALAMOS NATIONAL LABORATORY
MS D438
LOS ALAMOS, NM 87545
O1CY ATTN S.P. GARY
O1CY ATTN J. BOROVSKY

SANDIA LABORATORIES
P.O. BOX 5800
ALBUQUERQUE, NM 87115
O1CY ATTN DOC CON FOR W. BROWN
O1CY ATTN DOC CON FOR A. THORNBROUGH
O1CY ATTN DOC CON FOR T. WRIGHT
O1CY ATTN DOC CON FOR D. DAHLGREN
O1CY ATTN DOC CON FOR 3141
O1CY ATTN DOC CON FOR SPACE PROJEC
CTV

SANDIA LABORATORIES
LIVERMORE LABORATORY
P.O. BOX 969
LIVERMORE, CA 94550
O1CY ATTN DOC CON FOR B. MURPHAY
O1CY ATTN DOC CON FOR T. COOK

OFFICE OF MILITARY APPLICATION
DEPARTMENT OF ENERGY
WASHINGTON, DC 20545
O1CY ATTN DOC CON DR. YO SONG

OTHER GOVERNMENT

INSTITUTE FOR TELECOM SCIENCES
NATIONAL TELECOMMUNICATIONS & INFO
ADMIN
BOULDER, CO 80303
O1CY ATTN D. CROMBIE
O1CY ATTN L. BERRY

NATIONAL OCEANIC & ATMOSPHERIC ADMIN
ENVIRONMENTAL RESEARCH LABORATORIES
DEPARTMENT OF COMMERCE
BOULDER, CO 80302
O1CY ATTN R. GRUBB
O1CY ATTN AERONOMY LAB G. REID

DEPARTMENT OF DEFENSE CONTRACTORS

AEROSPACE CORPORATION
P.O. BOX 92957
LOS ANGELES, CA 90009
O1CY ATTN I. GARFUNKEL
O1CY ATTN T. SALMI
O1CY ATTN V. JOSEPHSON
O1CY ATTN S. BOWER
O1CY ATTN D. OLSEN

ANALYTICAL SYSTEMS ENGINEERING CORP
5 OLD CONCORD ROAD
BURLINGTON, MA 01803
O1CY ATTN RADIO SCIENCES

AUSTIN RESEARCH ASSOC., INC.
1901 RUTLAND DRIVE
AUSTIN, TX 78758
O1CY ATTN L. SLOAN
O1CY ATTN R. THOMPSON

BERKELEY RESEARCH ASSOCIATES, INC.
P.O. BOX 983
BERKELEY, CA 94701
O1CY ATTN J. WORKMAN
O1CY ATTN C. PRETTIE
O1CY ATTN S. BRECHT

BOEING COMPANY, THE
P.O. BOX 3707
SEATTLE, WA 98124
O1CY ATTN G. KEISTER
O1CY ATTN D. MURRAY
O1CY ATTN G. HALL
O1CY ATTN J. KENNEY

CHARLES STARK DRAPER LABORATORY, INC.
555 TECHNOLOGY SQUARE
CAMBRIDGE, MA 02139
O1CY ATTN D.B. COX
O1CY ATTN J.P. GILMORE

COMSAT LABORATORIES
LINTHICUM ROAD
CLARKSBURG, MD 20734
O1CY ATTN G. HYDE

CORNELL UNIVERSITY
DEPARTMENT OF ELECTRICAL ENGINEERING
ITHACA, NY 14850
O1CY ATTN D.T. FARLEY, JR.

ELECTROSPACE SYSTEMS, INC.
BOX 1359
RICHARDSON, TX 75080
O1CY ATTN H. LOGSTON
O1CY ATTN SECURITY (PAUL PHILLIPS)

EOS TECHNOLOGIES, INC.
606 Wilshire Blvd.
Santa Monica, CA 90401
O1CY ATTN C.B. GABBARD
O1CY ATTN R. LELEVIER

ESL, INC.
495 JAVA DRIVE
SUNNYVALE, CA 94086
O1CY ATTN J. ROBERTS
O1CY ATTN JAMES MARSHALL

GENERAL ELECTRIC COMPANY
SPACE DIVISION
VALLEY FORCE SPACE CENTER
GODDARD BLVD KING OF PRUSSIA
P.O. BOX 5555
PHILADELPHIA, PA 19101
O1CY ATTN M.H. BORTNER
SPACE SCI LAB

GENERAL ELECTRIC TECH SERVICES
CO., INC.
HMES
COURT STREET
SYRACUSE, NY 13201
O1CY ATTN G. MILLMAN

GEOPHYSICAL INSTITUTE
UNIVERSITY OF ALASKA
FAIRBANKS, AK 99701
(ALL CLASS ATTN: SECURITY OFFICER)
O1CY ATTN T.N. DAVIS (UNCLASS ONLY)
O1CY ATTN TECHNICAL LIBRARY
O1CY ATTN NEAL BROWN (UNCLASS ONLY)

GTE SYLVANIA, INC.
ELECTRONICS SYSTEMS GRP-EASTERN DIV
77 A STREET
NEEDHAM, MA 02194
O1CY ATTN DICK STEINHOF

HSS, INC.
2 ALFRED CIRCLE
BEDFORD, MA 01730
O1CY ATTN DONALD HANSEN

ILLINOIS, UNIVERSITY OF
107 COBLE HALL
150 DAVENPORT HOUSE
CHAMPAIGN, IL 61820
(ALL CORRES ATTN DAN MCCLELLAND)
O1CY ATTN K. YEH

INSTITUTE FOR DEFENSE ANALYSES
1801 NO. BEAUREGARD STREET
ALEXANDRIA, VA 22311
O1CY ATTN J.M. ABIN
O1CY ATTN ERNEST BAUER
O1CY ATTN HANS WOLFARD
O1CY ATTN JOEL BENGSTON

INT'L TEL & TELEGRAPH CORPORATION
500 WASHINGTON AVENUE
MUTLEY, NJ 07040
O1CY ATTN TECHNICAL LIBRARY

JAYCOR
11011 TORREYANA ROAD
P.O. BOX 85154
SAN DIEGO, CA 92138
O1CY ATTN J.L. SPERLING

JOHNS HOPKINS UNIVERSITY
APPLIED PHYSICS LABORATORY
JOHNS HOPKINS ROAD
LAUREL, MD 20810
O1CY ATTN DOCUMENT LIBRARIAN
O1CY ATTN THOMAS POTEYRA
O1CY ATTN JOHN DASSOULAS

KAMAN SCIENCES CORP
P.O. BOX 7463
COLORADO SPRINGS, CO 80933
O1CY ATTN T. MEAGHER

KAMAN TEMPO-CENTER FOR ADVANCED
STUDIES
816 STATE STREET P.O DRAWER QG
SANTA BARBARA, CA 93102
O1CY ATTN DASIAC
O1CY ATTN WARREN S. KNAPP
O1CY ATTN WILLIAM McNAMARA
O1CY ATTN B. GAMBILL

LINKABIT CORP
10453 ROSELLE
SAN DIEGO, CA 92121
O1CY ATTN IRWIN JACOBS

LOCKHEED MISSILES & SPACE CO., INC
P.O. BOX 504
SUNNYVALE, CA 94088
O1CY ATTN DEPT 60-12
O1CY ATTN D.R. CHURCHILL

LOCKHEED MISSILES & SPACE CO., INC.
3251 HANOVER STREET
PALO ALTO, CA 94304
O1CY ATTN MARTIN WALT DEPT 52-12
O1CY ATTN W.L. IMHOFF DEPT 52-12
O1CY ATTN RICHARD J. JOHNSON
DEPT 52-12
O1CY ATTN J.B. GLADIS DEPT 52-12

MARTIN MARIETTA CORP
ORLANDO DIVISION
P.O. BOX 5827
ORLANDO, FL 32805
O1CY ATTN R. REFFNER

MCDONNELL DOUGLAS CORPORATION
5301 BOLSA AVENUE
HUNTINGTON BEACH, CA 92647
O1CY ATTN N. HARRIS
O1CY ATTN J. MOULE
O1CY ATTN GEORGE MROZ
O1CY ATTN W. OLSON
O1CY ATTN R.W. HALPRIN
O1CY ATTN TECHNICAL
LIBRARY SERVICES

MISSION RESEARCH CORPORATION
735 STATE STREET
SANTA BARBARA, CA 93101
O1CY ATTN P. FISCHER
O1CY ATTN W.F. CREVIER
O1CY ATTN STEVEN L. GUTSCHE
O1CY ATTN R. BOGUSCH
O1CY ATTN R. HENDRICK
O1CY ATTN RALPH KILB
O1CY ATTN DAVE SOWLE
O1CY ATTN F. FAJEN
O1CY ATTN M. SCHEIBE
O1CY ATTN CONRAD L. LONGMIRE
O1CY ATTN B. WHITE
O1CY ATTN R. STAGAT

MISSION RESEARCH CORP.
1720 RANDOLPH ROAD, S.E.
ALBUQUERQUE, NM 87106
O1CY R. STELLINGWERF
O1CY M. ALME
O1CY L. WRIGHT

MITRE CORP
WESTGATE RESEARCH PARK
1820 DOLLY MADISON BLVD
MCLEAN, VA 22101
O1CY ATTN W. HALL
O1CY ATTN W. FOSTER

PACIFIC-SIERRA RESEARCH CORP
12340 SANTA MONICA BLVD.
LOS ANGELES, CA 90025
O1CY ATTN E.C. FIELD, JR.

PENNSYLVANIA STATE UNIVERSITY
IONOSPHERE RESEARCH LAB
318 ELECTRICAL ENGINEERING EAST
UNIVERSITY PARK, PA 16802
(NO CLASS TO THIS ADDRESS)
O1CY ATTN IONOSPHERIC RESEARCH LAB

PHOTOMETRICS, INC.
4 ARROW DRIVE
WOBURN, MA 01801
O1CY ATTN IRVING L. KOFSKY

PHYSICAL DYNAMICS, INC.
P.O. BOX 3027
BELLEVUE, WA 98009
O1CY ATTN E.J. FREMOUW

PHYSICAL DYNAMICS, INC.
P.O. BOX 10367
OAKLAND, CA 94610
ATTN A. THOMSON

R & D ASSOCIATES
P.O. BOX 9695
MARINA DEL REY, CA 90291
O1CY ATTN FORREST GILMORE
O1CY ATTN WILLIAM B. WRIGHT, JR.
O1CY ATTN WILLIAM J. KARZAS
O1CY ATTN H. ORY
O1CY ATTN C. MACDONALD

RAND CORPORATION, THE
15450 COHASSET STREET
VAN NUYS, CA 91406
O1CY ATTN CULLEN CRAIN
O1CY ATTN ED BEDROZIAN

RAYTHEON CO.
528 BOSTON POST ROAD
SUDBURY, MA 01776
O1CY ATTN BARBARA ADAMS

RIVERSIDE RESEARCH INSTITUTE
330 WEST 42nd STREET
NEW YORK, NY 10036
O1CY ATTN VINCE TRAPANI

SCIENCE APPLICATIONS, INC.
1150 PROSPECT PLAZA
LA JOLLA, CA 92037
O1CY ATTN LEWIS M. LINSON
O1CY ATTN DANIEL A. HAMLIN
O1CY ATTN E. FRIEMAN
O1CY ATTN E.A. STRAKER
O1CY ATTN CURTIS A. SMITH

SCIENCE APPLICATIONS, INC
1710 GOODRIDGE DR.
MCLEAN, VA 22102
O1CY J. COCKAYNE
O1CY E. HYMAN

SRI INTERNATIONAL
333 RAVENSWOOD AVENUE
MENLO PARK, CA 94025
01CY ATTN J. CASPER
01CY ATTN DONALD NEILSON
01CY ATTN ALAN BURNS
01CY ATTN G. SMITH
01CY ATTN R. TSUNODA
01CY ATTN DAVID A. JOHNSON
01CY ATTN WALTER G. CHESNUT
01CY ATTN CHARLES L. RINO
01CY ATTN WALTER JAYE
01CY ATTN J. VICKREY
01CY ATTN RAY L. LEADABRAND
01CY ATTN G. CARPENTER
01CY ATTN G. PRICE
01CY ATTN R. LIVINGSTON
01CY ATTN V. GONZALES
01CY ATTN D. McDANIEL

TECHNOLOGY INTERNATIONAL CORP
75 WIGGINS AVENUE
BEDFORD, MA 01730
01CY ATTN W.P. BOQUIST

TRW DEFENSE & SPACE SYS GROUP
ONE SPACE PARK
REDONDO BEACH, CA 90278
01CY ATTN R. K. PLEBUCH
01CY ATTN S. ALTSCHULER
01CY ATTN D. DEE
01CY ATTN D/ STOCKWELL
SNTF/1575

VISIDYNE
SOUTH BEDFORD STREET
BURLINGTON, MA 01803
01CY ATTN W. REIDY
01CY ATTN J. CARPENTER
01CY ATTN C. HUMPHREY

UNIVERSITY OF PITTSBURGH
PITTSBURGH, PA 15213
01CY ATTN: N. ZABUSKY

DTIC
02CY

CODE 1220
01CY

DIRECTOR OF RESEARCH
U.S. NAVAL ACADEMY
ANNAPOLIS, MD 21402
02CY

IONOSPHERIC MODELING DISTRIBUTION LIST
(UNCLASSIFIED ONLY)

PLEASE DISTRIBUTE ONE COPY TO EACH OF THE FOLLOWING PEOPLE (UNLESS OTHERWISE NOTED)

NAVAL RESEARCH LABORATORY
WASHINGTON, DC 20375

DR. H. GURSKY - CODE 4100
DR. P. GOODMAN - CODE 4180
Dr. P. RODRIQUEZ - CODE 4706

A.F. GEOPHYSICS LABORATORY

L.G. HANSCOM FIELD
BEDFORD, MA 01731
DR. T. ELKINS
DR. W. SWIDER
MRS. R. SAGALYN
DR. J.M. FORBES
DR. T.J. KENESHEA
DR. W. BURKE
DR. H. CARLSON
DR. J. JASPERS
Dr. F.J. RICH
DR. N. MAYNARD

BOSTON UNIVERSITY
DEPARTMENT OF ASTRONOMY
BOSTON, MA 02215
DR. J. AARONS

CORNELL UNIVERSITY
ITHACA, NY 14850
DR. W.E. SWARTZ
DR. D. FARLEY
DR. M. KELLEY

HARVARD UNIVERSITY
HARVARD SQUARE
CAMBRIDGE, MA 02138
DR. M.B. McELROY
DR. R. LINDZEN

INSTITUTE FOR DEFENSE ANALYSIS
1801 N. BEAUREGARD STREET
ARLINGTON, VA 22311
DR. E. BAUER

MASSACHUSETTS INSTITUTE OF
TECHNOLOGY
PLASMA FUSION CENTER
LIBRARY, NW16-262
CAMBRIDGE, MA 02139

NASA
GODDARD SPACE FLIGHT CENTER
GREENBELT, MD 20771
DR. N. MAYNARD (CODE 696)
DR. K. MAEDA
DR. S. CURTIS
DR. M. DUBIN

COMMANDER
NAVAL AIR SYSTEMS COMMAND
DEPARTMENT OF THE NAVY
WASHINGTON, DC 20360
DR. T. CZUBA

COMMANDER
NAVAL OCEAN SYSTEMS CENTER
SAN DIEGO, CA 92152
MR. R. ROSE - CODE 5321

NOAA
DIRECTOR OF SPACE AND
ENVIRONMENTAL LABORATORY
BOULDER, CO 80302
DR. A. GLENN JEAN
DR. G.W. ADAMS
DR. D.N. ANDERSON
DR. K. DAVIES
DR. R.F. DONNELLY

OFFICE OF NAVAL RESEARCH
800 NORTH QUINCY STREET
ARLINGTON, VA 22217
DR. G. JOINER

LABORATORY FOR PLASMA AND
FUSION ENERGIES STUDIES
UNIVERSITY OF MARYLAND
COLLEGE PARK, MD 20742
JHAN VARYAN HELLMAN,
REFERENCE LIBRARIAN

PENNSYLVANIA STATE UNIVERSITY
UNIVERSITY PARK, PA 16802
DR. J.S. NISBET
DR. P.R. ROHRBAUGH
DR. L.A. CARPENTER
DR. M. LEE
DR. R. DIVANY
DR. P. BENNETT
DR. F. KLEVANS

SCIENCE APPLICATIONS, INC.
1150 PROSPECT PLAZA
LA JOLLA, CA 92037
DR. D.A. HAMLIN
DR. E. FRIEMAN

STANFORD UNIVERSITY
STANFORD, CA 94305
DR. P.M. BANKS

U.S. ARMY ABERDEEN RESEARCH
AND DEVELOPMENT CENTER
BALLISTIC RESEARCH LABORATORY
ABERDEEN, MD
DR. J. HEIMERL

GEOPHYSICAL INSTITUTE
UNIVERSITY OF ALASKA
FAIRBANKS, AK 99701
DR. L.E. LEE

UNIVERSITY OF CALIFORNIA
LOS ALAMOS NATIONAL LABORATORY
J-10, MS-664
LOS ALAMOS, NM 87545
DR. M. PONGRATZ
DR. D. SIMONS
DR. G. BARASCH
DR. L. DUNCAN
DR. P. BERNHARDT
DR. S.P. GARY

UNIVERSITY OF MARYLAND
COLLEGE PARK, MD 20740
DR. K. PAPADOPOULOS
DR. E. OTT

JOHNS HOPKINS UNIVERSITY
APPLIED PHYSICS LABORATORY
JOHNS HOPKINS ROAD
LAUREL, MD 20810
DR. R. GREENWALD
DR. C. MENG

UNIVERSITY OF PITTSBURGH
PITTSBURGH, PA 15213
DR. N. ZABUSKY
DR. M. BIONDI
DR. E. OVERMAN

UNIVERSITY OF TEXAS
AT DALLAS
CENTER FOR RESEARCH SCIENCES
P.O. BOX 688
RICHARDSON, TX 75080
DR. R. HEELIS
DR. W. HANSON
DR. J.P. McCLURE

UTAH STATE UNIVERSITY
4TH AND 8TH STREETS
LOGAN, UT 84322
DR. R. HARRIS
DR. K. BAKER
DR. R. SCHUNK
DR. J. ST.-MAURICE

PHYSICAL RESEARCH LABORATORY
PLASMA PHYSICS PROGRAMME
AHMEDABAD 380 009
INDIA

P.J. PATHAK, LIBRARIAN
LABORATORY FOR PLASMA AND
FUSION ENERGY STUDIES
UNIVERSITY OF MARYLAND
COLLEGE PARK, MD 20742
JHAN VARYAN HELLMAN,
REFERENCE LIBRARIAN

UNIVERSITY OF ILLINOIS
DEPT. OF ELECTRICAL ENGINEERING
1406 W. GREEN STREET
URBANA, IL 61801
DR. ERHAN KUDEKI

END

FILMED

5-86

DTIC